Pis'ma v ZhETF, vol. 100, iss. 5, pp. 390 – 393

Two models of anisotropic propagation of cardiac excitation wave

I. S. Erofeev, K. I. Agladze[1)]

Laboratory of Biophysics of Excitable Systems, Moscow Institute of Physics and Technology, 141700 Dolgoprudny, Russia

Submitted 30 July 2014

Propagation of the action potential in the real heart is direction-dependent (anisotropic). We propose two general physical models explaining this anisotropy on the cellular level. The first, "delay" model takes into account the frequency of the cell–cell transitions in different directions of propagation, assuming each transition requires some small time interval. The second model relies on the assumption that the action potential transmits to the next cell only from the area at the pole of the previous cell. We estimated parameters of both models by doing optical mapping and fluorescent staining of cardiac cell samples grown on polymer fiber substrate. Both models gave reasonable estimations, but predicted different behavior of anisotropy ratio (ratio of largest and smallest wave velocities) after addition of sodium channels supressor like lidocaine. The results of the experiment on lidocaine effect on anisotropy ratio was in favor of the first, "delay" model. Estimated average cell–cell transition delay was $240 \pm 80\,\mu$s, which is close to the characteristic values of synaptic delay.

DOI: 10.7868/S0370274X14170123

1. Introduction. Cardiac cells are capable to generate an action potential (AP) as well as transmit it in a form of propagating excitation wave [1]. Understanding the mechanisms of the excitation propagation in a heart is extremely important due to its relation to the normal–abnormal heart functioning and origins of lethally dangerous arrhythmia [2]. The existence of the excitation wave is provided by two processes: local generation and propagation of AP. Excitation generation constitutes a rapid change in the membrane potential, and is based on the work of voltage-gated ion channels. Propagation of the AP throughout the excitable network, from cell to cell, relies on the connections between the cells: gap-junctions, electrotonic connections, etc. [3, 4]. In the isotropic cell layers of the cultured cardiac tissue, where cells are distributed randomly without preferred orientation, the AP propagates similar to the excitation waves in the Belousov–Zhabotinsky reaction in a circular or spiral shape [5]. However, the real cardiac tissue is essentially anisotropic, representing a complex structure of the myofibrils where elongated cardiac cells are packed in the compact bunches. In a cultured cardiac tissue, such anisotropic structure may primitively be mimicked by seeding cardiac cells on the aligned polymer nanofibers, guiding cell shape and development [6]. This simplified experimental model gives at least one important feature of the anisotropic cardiac tissue: the propagation of excitation along the axis of alignment is much faster than across it [6–8], Fig. 1.

[1)]e-mail: agladze@yahoo.com

Although, well documented on a macro-level, this anisotropy of the excitation propagation has little supporting data involving processes on the cell-level scale. Most mathematical models neglect the discrete nature of real cardiac tissue [9–12]. When anisotropy is essential in modeling excitation propagation, a set (a tensor) of empirical conduction coefficients is generally used [13]. In this work we are making an attempt to approach the propagation of excitation from the cellular level employing relatively simple physical principles and marking the direction in which further study should focus.

1.1. Two models employed. The proposed two models are based on the following same assumptions: the characteristics of voltage-gated ion channels (more precisely, fast sodium channels) responsible for the AP generations are the same in any location within the cell and do not depend on the shape of the cell. The propagation of the AP involves two processes: propagation in the cell membrane within a single cell and the AP transmission from cell to cell. The difference between the models is in the mechanisms underlying the anisotropic excitation propagation in the aligned cell culture.

The first model (*"delay" model*) takes into account the frequency of the cell–cell transitions in different directions of propagation, whereas the transitions may happen at any locations in the cell which are in contact with the neighboring cells. The cell–cell transitions retard wave propagation by the fixed interval of time each, and consequently the propagation is slower in the direction where more transitions are passed, Fig. 2a.

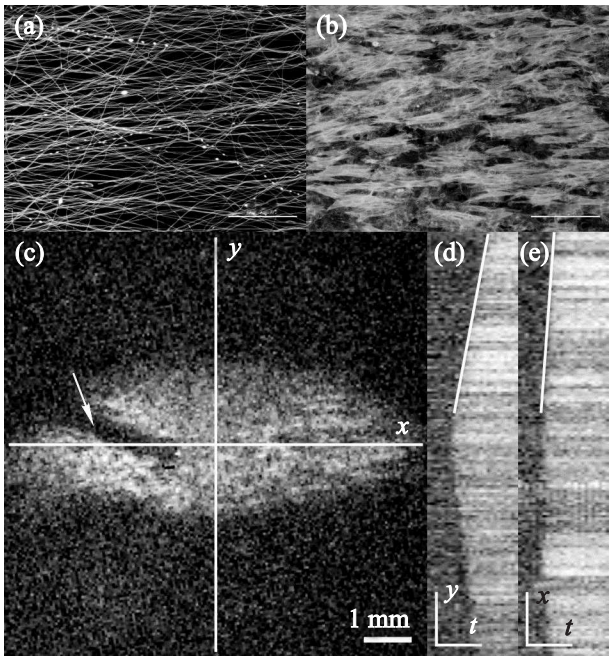

Fig. 1. Top row: confocal microscope images of cardiac cells grown on aligned nanofiber substrate. (a) – PCL nanofibers stained with rhodamine (b) cells, stained for α-actin. One can see correlated elongation of fibers and cells. Bottom row: anisotropy of wave propagation on cardiac cell sample as consequence of preferred elongation direction of cells. (c) – Optical mapping image of wave propagation. Cells were stimulated from the center. Wavefront velocity along x-axis is greater than along y-axis. Thus the wavefront has an elliptic form. Arrow depicts the shadow from the electrode. (d, e) – Time-space plots of y- and x-axes. Wavefront line slope shows the wavefront speed

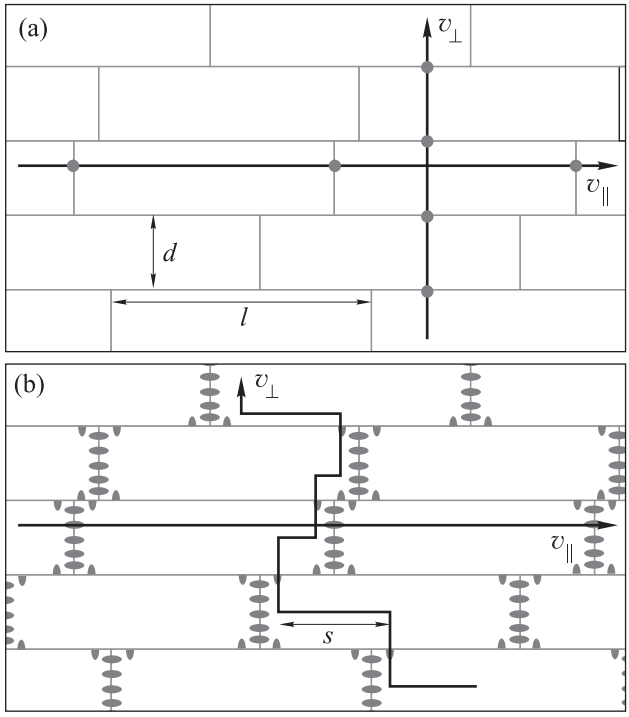

Fig. 2. Two models of anisotropic AP propagation. (a) – According to "delay" model, wave propagation speed depends on the linear density of cell–cell transitions, where delays take place. (b) – Following "deviated path" model, cell–cell transitions can happen only from cell poles. In that case transversal wave path is more twisted, and average wave speed is smaller

Namely, anisotropy emerges due to delays in wave propagation when it transits from one cell to another. The linear density of cell contacts is different along longitudal (along fibers) and transversal (across fibers) directions. The estimates for the longitudinal $v_\parallel$ and transversal $v_\perp$ velocities can be done as follows:

$$v_\parallel = \frac{v_0}{1 + v_0\tau/l}, \quad v_\perp = \frac{v_0}{1 + v_0\tau/d},$$

where v_0 – wavefront velocity along cell itself, τ – delay time, l – mean longitudinal length of cells, d – mean transversal length (width) of cells. If τ is negligibly small, the velocity does not depend on the direction of propagation. Contrary, if τ is very large, and we can neglect the time when AP propagates over the single cell, the ratio of velocities will be an inverse ratio of the cell width to the cell length.

The second model (*"deviated path" model*) relies on the assumption that the AP transmits to the next cell only from the area at the pole of the previous cell. This effect results from uneven distribution of the voltage-gated ion channels, it was reported that the fast sodium channels are distributed preferentially at the poles of the cardiomyocyte [14, 15]. Consequently, although the density of the sodium channels between cell poles is sufficient for the AP propagation intracellularly, one can assume that the current density required for transmission of AP from cell to cell can be reached only at the cell poles. Thus, the excitation path alters from the shortest direct line, especially in the direction perpendicular to the alignment axis, Fig. 2b. In that case wave propagates along the fibers directly with the velocity $v_\parallel = v_0$. However, in transversal direction, wave path changes since the excitation needs to reach the cell pole before it transits further. If on average wave travels distance s in longitudinal direction before it transits to the next cell, the estimation of transversal velocity is

$$v_\perp = \frac{v_0}{1 + s/d}.$$

Mean distance s depends on the geometry of the sample and can be estimated as $s = \alpha l$, where $\alpha = 0.1{-}0.3$

from common sense. In the simple case of rectangular randomly shifted cells $\alpha = 0.25$.

Summarizing, the main qualitative difference between two models constitutes in following. While in the first model the ratio of longitudinal and transversal velocities may depend on the particular dynamics of excitation, which would reflect the different ratio of τ and v_0, in the second model the velocity ratio depends only on geometrical parameters. This qualitative difference between the models gives us an instrument to verify their applicability.

2. Experimental verification. *2.1. Materials and methods.* Primary cell cultures of neonatal rat ventricular myocytes were prepared as described in [16]. Briefly, hearts were removed from 1- to 2-day-old Wistar rats anesthetized by isoflurane. The hearts were minced and digested in PBS containing 0.2 % collagenase type I. The isolated cells were collected by centrifugation and incubated in 100-mm cell culture dishes for 1 h at 37 °C in a humidified incubator with 5 % CO_2 air. After supernatant was collected again, the cells were seeded into 22-mm diameter coverslips coated with fibronectin (16.7 g/ml) at a cell density of $2.6 \cdot 10^3$ cells/mm^2. The cells were incubated in Dulbecco-modified Eagle medium supplemented with 10 % fetal bovine serum and 1 % penicillin streptomycin. After 24 h, the medium was replaced with minimum essential medium supplemented with 10 % calf serum and 1 % penicillin streptomycin, and the cells were incubated under the same condition. To monitor activity and visualize the excitation wave propagation, the cells were loaded with the Ca^{2+} sensitive indicator Fluo-4-AM (Invitrogen, USA) in Tyrode solution at room temperature. After staining (35 min), the medium was exchanged with fresh Tyrode solution (Sigma-Aldrich Co., USA) and kept at room temperature during the observations. The excitation waves were monitored using a high-speed imaging setup (an Olympus MVX-10 microscope equipped with EM-CCD camera, Andor iXon3). Images were acquired at 68 fps. To measure average cell size, cell samples were stained for α-actin with Alexa Fluor 488 Phalloidin Conjugate and incubated for 1 h. After staining, the samples were rinsed with PBS and mounted on a glass slide with Vectashield Mounting Medium containing DAPI, which stained nuclei. Fluorescent images were recorded with Zeiss Confocal microscope L710.

2.2. Results. First, we estimated the shape of the aligned cells, Fig. 3. And measured the propagation velocities in longitudinal and transversal directions. Accordingly, mean cell size was: $d \times l = 17 \times 77\,\mu$m, and the corresponding velocities were: $v_\perp = 75 \pm 2$ mm/s,

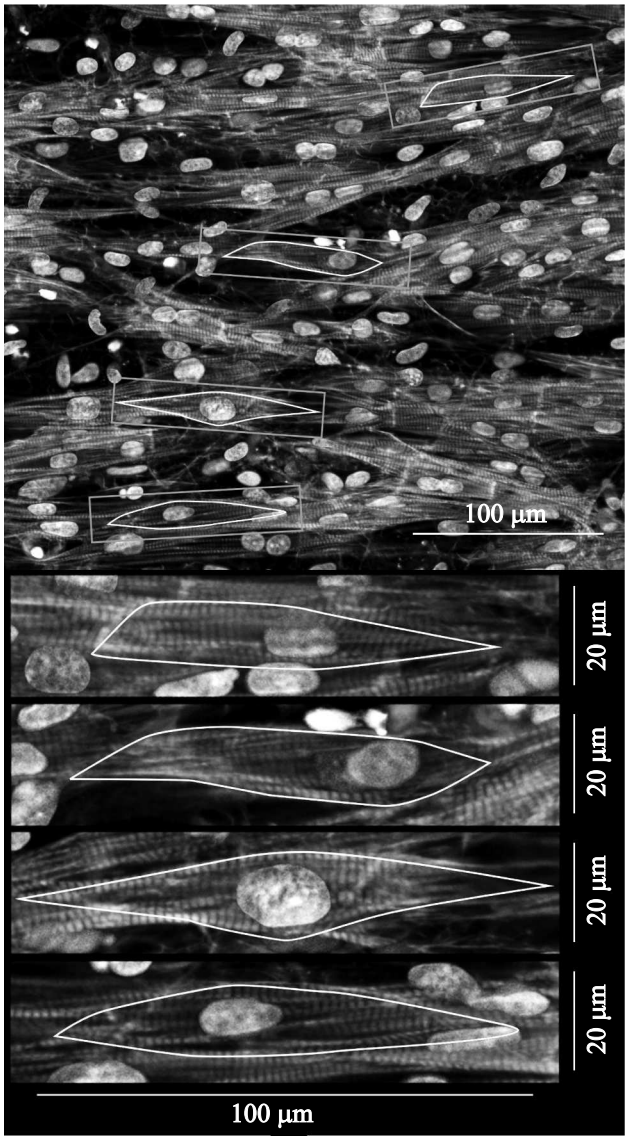

Fig. 3. Confocal image of aligned cell culture (α-actin fibers and cell nuclei). Borders of four cells are shown. Estimated mean width and length of the cell are $17 \times 77\,\mu$m^2

$v_\parallel = 41 \pm 1$ mm/s. For the first, "delay" model parameters v_0 and τ could be estimated from the system:

$$v_\parallel^{-1} = v_0^{-1} + \tau l^{-1},$$
$$v_\perp^{-1} = v_0^{-1} + \tau d^{-1}.$$

Which gives $v_0 = 98 \pm 14$ mm/s, $\tau = 240 \pm 80\,\mu$s. For the "deviated pathway" model we have $v_0 = v_\parallel = 75 \pm \pm 2$ mm/s. From $v_0/v_\perp = 1 + \alpha l/d$ we get $\alpha = 0.18 \pm 0.05$ which correlates with first estimations of α.

At this point, it is impossible to distinguish between the two models, as both estimations look reasonable. However, as said above, the anisotropy ratio for the first model (AR, the ratio of longitudinal and transver-

Lidocaine effect on anisotropy ratio

Lidocaine concentration, μm	Longitudal velocity, mm/s	Transversal velocity, mm/s	Anisotropy ratio (AR)
0	112 ± 2	46.0 ± 1.2	2.43 ± 0.11
100	27.2 ± 0.9	13.3 ± 0.7	2.04 ± 0.16

sal velocities) should depend on the local ion channel kinetics, which changes v_0 and does not affect τ. For modulating the activity of the fast sodium channels we added lidocaine [17, 18]. If the "delay" model is valid, the transversal velocity should decrease less than longitudinal one, which would lead to a decrease of the AR. On the contrary, according to "deviated path" model, the addition of the lidocaine would not change the AR since it is dependent only on the cell shape. The results of the AR measurement are summarized in the Table.

3. Conclusion. The decrease of the anisotropy ratio under the lidocaine evidences for the validity of the first model. Interestingly, the value of τ around 240 μs is close to the characteristic values of synaptic delay which is time (typically 0.3–0.5 ms) required for a neurotransmitter to be released from a presynaptic membrane, diffuse across the synaptic cleft, and bind to a receptor site on the post-synaptic membrane [19, 20]. Thus, our data indicate that cell to cell transmission of excitation in cardiac cells may involve relatively slow processes, most probably limited in speed by the diffusion of ionic currents particle (ions) or related to the capacitive properties of the cell membrane. The precise nature of cell–cell delay in the propagation of cardiac excitation will be a subject of our future studies, involving high resolution optical mapping of two connected cardiac cells.

Authors would like to offer special thanks to Alexander Teplenin for help with polymer fiber substrate preparation. The research was partially supported by Federal "5top100" Program.

1. V. I. Krinsky, V. N. Biktashev, and A. M. Pertsov, Ann. NY Acad. Sci. **591**, 232 (1990).
2. M. Vaquero, D. Calvo, and J. Jalife, Heart Rhythm **5**(6), 872 (2008).
3. A. G. Kleber and Y. Rudy, Phys. Rev. **84**(2), 431 (2004).
4. P. Colli-Franzone, L. F. Pavarino, and B. Taccardi, Math. Biosci. Eng. **197**(1), 35 (2005).
5. A. T. Winfree, Sci. Am. **230**(6), 82 (1974).
6. Y. Orlova, N. Magome, L. Liu, Y. Chen, and K. Agladze, Biomaterials **32**(24), 5615 (2011).
7. N. Bursac, Y. H. Loo, K. Leong, and L. Tung, Biochem. Bioph. Res. Co. **361**(4), 847 (2007).
8. N. Bursac, K. K. Parker, S. Iravanian, and L. Tung, Circ. Res. **91**(12), e45 (2002).
9. V. N. Biktashev, A. V. Holden, S. F. Mironov, A. M. Pertsov, and A. V. Zaitsev, J. Physiol.-London **9**(04), 695 (1998).
10. F. Fenton and A. Karma, Chaos **8**(1), 20 (1998).
11. C. F. Starmer, V. N. Biktashev, D, N. Romashko, M. R. Stepanov, O. N. Makarova, and V. I. Krinsky, Biophys. J. **65**(5), 1775 (1993).
12. V. I. Krinsky, Pharmacol. Ther. B **3**(4), 539 (1978).
13. R. L. Winslow, D. F. Scollan, A. Holmes, C. K. Yung, J. Zhang, and M. S. Jafri, Annu. Rev. Biomed. Eng. **2**, 119 (2000).
14. A. S. Amin, H. L. Tan, and A. A. M. Wilde, Heart Rhythm **7**(1), 117 (2010).
15. A. Bhargava, X. Lin, P. Novak, K. Mehta, Y. Korchev, M. Delmar, and J. Gorelik, Circ. Res. **112**(8), 1112 (2013).
16. K. Agladze, M. W. Kay, V. Krinsky, and N. Sarvazyan, Am. J. Physiol-Heart C. **293**, 503 (2007).
17. A. Isomura, M. Hörning, K. Agladze, and K. Yoshikawa, Phys. Rev. E **78**, 1 (2008).
18. S. Kadota, M. W. Kay, M. Magome, and K. Agladze, JETP Lett. **94**(11), 824 (2012).
19. J. D. Clements, Trends Neurosci. **19**(5), 163 (1996).
20. B. Katz and R. Miledi, J. Physiol. **231**(3), 549 (1973).